R-10-58

The potential for methane hydrate formation in deep repositories of spent nuclear fuel in granitic rocks

Bahman Tohidi, Antonin Chapoy
Hydrafact Ltd, Institute of Petroleum Engineering,
Heriot-Watt University, Edinburgh

John Smellie, Conterra AB

Ignasi Puigdomenech, Svensk Kärnbränslehantering AB

December 2010

Svensk Kärnbränslehantering AB
Swedish Nuclear Fuel
and Waste Management Co

Box 250, SE-101 24 Stockholm
Phone +46 8 459 84 00

ISSN 1402-3091
SKB R-10-58

The potential for methane hydrate formation in deep repositories of spent nuclear fuel in granitic rocks

Bahman Tohidi, Antonin Chapoy
Hydrafact Ltd, Institute of Petroleum Engineering,
Heriot-Watt University, Edinburgh

John Smellie, Conterra AB

Ignasi Puigdomenech, Svensk Kärnbränslehantering AB

December 2010

Keywords: Methane, Clathrate, Groundwater, Permafrost, SKBdoc 1264075.

Summary

The main aim of this work was to establish whether the pertaining pressure and temperature conditions and dissolved gas concentration in groundwater is conducive to gas hydrate formation using a modelling approach.

The hydrate stability pressure-temperature zone of dissolved methane in the presence of salt has been obtained through calculations which show that a decrease in the system pressure and/or an increase in salt concentration favours hydrate formation, as both factors reduce equilibrium gas solubility in the aqueous phase. This behaviour is unlike that of the system including a gas phase, where the water phase is always saturated with methane, and hence the methane solubility in water is not a limiting factor.

The main conclusion is that hydrate formation is not possible at the reported methane concentrations and water salinities for the Forsmark and Laxemar sites in Sweden and Olkiluoto in Finland. At the highest salinities and methane concentrations encountered, namely ~0.00073 mole fraction methane and ~10 mass % NaCl at a depth of 1,000 m in Olkiluoto, Finland, hydrates could form if the system temperatures and pressures are below 2.5°C and 60 bar, respectively, i.e. values that are much lower than those prevailing at that depth (~20°C and ~100 bar, respectively).

Furthermore, the calculated results provide the necessary data to estimate the effect of increase in dissolved methane concentration on potential hydrate formation, as well as two phase flow.

The available depth dependency of methane concentration at the sites studied in Sweden and Finland was used in another study to estimate the diffusive flow of methane in the rock volumes. These diffusion rates, which are highest at Olkiluoto, indicate that even if the conditions were to become favourable to methane hydrate formation, then it would take several millions of years before a thin layer of hydrates could be formed, a condition which is outside the required period of satisfactory performance of spent nuclear fuel repositories, namely ~1 million years.

Contents

1 Introduction and objectives

Underground storage is one of the options being considered in Sweden and Finland for the safe disposal of spent nuclear fuel. Two sites in Sweden and four sites in Finland have been investigated for this purpose. The selected site in Sweden by SKB (Swedish Nuclear Fuel and Waste Management Co.) is that of Forsmark, while the selected site by Posiva Oy in Finland is that of Olkiluoto.

Climate modelling shows that these Fennoscandian sites will undergo significant climate changes in the next 120,000 years, including glaciation with an ice thickness of perhaps up to two thousand metres. The presence of underground water with dissolved hydrocarbon gases, combined with low temperature and high pressure conditions associated with glaciations, could result in gas hydrate formation. Natural gas hydrates comprise solid crystalline compounds composed of molecules of natural gas trapped in cages of hydrogen-bonded water molecules (i.e. clathrates). Gas hydrates are commonly present in and below current permafrost regions (e.g. MacKenzie Delta, northern Canada /Dallimore and Collett 1995, 1999/) and it is conceivable that if the area of permafrost expands during possible future periglacial periods, methane gas hydrate formation may take place under the permafrost layer due to lower temperatures even without the nuclear waste disposal sites being buried by glaciers. An additional factor which may influence methane hydrate stability is the presence of dissolved salts (e.g. saline groundwaters); thermodynamically, the main effect on the three phase equilibrium will be to lower the free energy of the water molecules in the liquid, thus inhibiting the formation of the methane hydrate.

At or near the bedrock surface the source of methane is usually biogenic in origin. At deeper levels it can be assumed that it is only in a few highly conductive fracture systems that a substantial upward transport and enrichment of methane, mostly abiogenic in origin, is possible. Methane hydrate could therefore form in reasonable quantities in the upper part of the bedrock with the onset of permafrost, and continue to form at increasing depth during permafrost conditions, its formation being restricted to the open fracture systems. The permafrost horizon effectively forms an impervious cap which may serve to trap, concentrate and convert into hydrates the methane gas that is transported upwards.

An eventual build up of methane gas hydrates above a potential repository for nuclear waste may give rise to some safety concerns during the expected lifespan of the repository, see for example /Bath and Hermansson 2009, Appendix C/. These include:

- Important hydrogeological and geochemical implications of methane hydrate formation. During permafrost periods there is the potential for sealing of porosity and fracture space, thus reducing bedrock permeability. The groundwater chemistry can be affected by the freeze-out of salts well below the extent of the permafrost, to the base of hydrate formation, because methane hydrates are stable well beneath the permafrost base.
- The dissociation of the solid methane hydrate phase to water/ice and methane gas (e.g. during warm periods), would achieve a volume change that could affect the rock, especially if large quantities are dissociated in a short period of time in a confined area. Although the porosity of the Fennoscandian granitic rocks of interest is too small for this process to be of importance, methane gas hydrates could be formed in sufficient large amounts in empty cavities within the nuclear repository constructions. The potentially large release of gas could then lead to a reduction in the strength of the bedrock hosting the repository, i.e. potentially increasing the groundwater flow in the upper part of the repository bedrock.
- In the context of a nuclear repository engineered barrier system, the melting of permafrost ice and gas hydrates may subsequently cause a dilution in groundwaters. Very dilute groundwaters will increase the stability of colloids derived from bentonite used as a buffer material to radionuclide transport. The removal of bentonite colloids during long periods of time by flowing groundwaters of very low ionic strength may affect the future performance of the nuclear repositories.

Faced with these concerns, the present study was initiated with the objective to assess the potential for gas hydrate formation and dissociation in deep (~500 m) underground storage of nuclear wastes in the three sites identified in the Swedish and Finnish Precambrian basement, i.e. Forsmark and Laxemar, and Olkiluoto, respectively.

2 Approach

A modelling approach was used to establish whether the pertaining pressure and temperature conditions and dissolved gas concentration in the bedrock groundwater are conducive to gas hydrate formation. However, because the pore size and contact angle will also affect the zone of hydrate stability, it was decided to look into potential hydrate formation in bulk conditions, as this represents the worst case scenario.

Thermodynamic modelling was carried out using the gas hydrate software 'Heriot-Watt Hydrate programme (HWHYD)' now licensed to 'Hydrafact' and renamed to 'HydraFLASH™'. Three versions exist: Version 1, Version 2.1 and the latest Version 2.2; Version 2.1 has been used in this report[1]. The full price for a Single User-Individual Licence for use in any one machine is 6,600 EUR (Set Up) + 1,100 EUR (Annual Upgrades, Debug and Support); there is the option for a Rental Licence for one year (renewable) for 2,650 EUR which includes set-up, annual upgrades, debug and support. The software has been evaluated independently by 'Total' (The French Oil Company) and judged the best software in its category.

The specific tasks were as follows:

- Predicting the solubility of gas in water in equilibrium with hydrates as a function of water salinity at a number of system pressures (50, 100, 150, 200, 250, and 300 bar) over a wide temperature range (i.e. −15 to +25 ºC). The results combined with the reported gas solubility data should demonstrate the potential for gas hydrate formation from dissolved gases.
- Knowing the system pressure and temperature, together with the gas content of the underground waters and their salinity, the potential for gas hydrate formation was evaluated.

[1] Please visit the following link for a full list of papers (all modelling papers are related to the software):

http://www.pet.hw.ac.uk/research/hydrate/publications.cfm

3 Description and validation of the thermodynamic model

3.1 Description

A general phase equilibrium model based on the uniformity of component fugacities in all phases has been used to model the phase behaviour of the methane-water system. A description of the thermodynamic model can be found elsewhere /Valderrama 1990/. In summary, the statistical thermodynamics model uses the Valderrama modification of the Patel and Teja equation of state (VPT-EoS) /Avlonitis et al. 1994/ and non-density-dependent mixing rules (NDD) for fugacity calculations in all fluid phases.

The VPT – EoS is given by:

$$P = \frac{RT}{v-b} - \frac{a\alpha(T_r)}{v(v+b)+c(v-b)}$$

The NDD mixing rules are applied to describe mixing in the *a*-parameter:

$a = a^C + a^A$

where a^C is given by the classical quadratic mixing rules as follows:

$$a^C = \sum_i \sum_j x_i x_j a_{ij}$$

and a_{ij} parameter is expressed by:

$$a_{ij} = (1-k_{ij})\sqrt{a_i a_j}$$

where k_{ij} is the standard binary interaction parameter (BIP).

The term a^A corrects for asymmetric interaction, which cannot be efficiently accounted for by classical mixing rules:

$$a^A = \sum_p x_p^2 \sum_i x_i a_{pi} l_{pi}$$

$$a_{pi} = \sqrt{a_p a_i}$$

$$l_{pi} = l_{pi}^0 - l_{pi}^1 (T - 273.15)$$

where *p* is the index of polar components and *l* is the binary interaction parameter for the asymmetric term.

The hydrate phase is modelled using the solid solution theory of /van der Waals and Platteeuw 1959/, as developed by /Parrish and Prausnitz 1972/. The equation recommended by /Holder et al. 1980/ is used to calculate the heat capacity difference between the empty hydrate lattice and pure liquid water. The Kihara model for spherical molecules is applied to calculate the potential function for compounds forming hydrate phases /Kihara 1953/.

3.2 Validations

The HWHYD model (cf. Chapter 2) has been previously evaluated for the methane–water system /Chapoy et al. 2004, Mohammadi et al. 2004, Najibi et al. 2009/. The main conclusions from this work are that the resulting thermodynamic model has been used for predicting CH_4 solubility in water, as well as water content of the CH_4-rich phase and finally the CH_4 hydrate phase equilibria over a wide range of temperature and pressure conditions. The predictions were found to be in good agreement with the experimental data, demonstrating the reliability of the model used in this work. Some of the predictions for hydrate phase equilibria of methane gas in the presence of distilled water (Figure 3-1) and various concentrations of NaCl (Figure 3-2) are presented below.

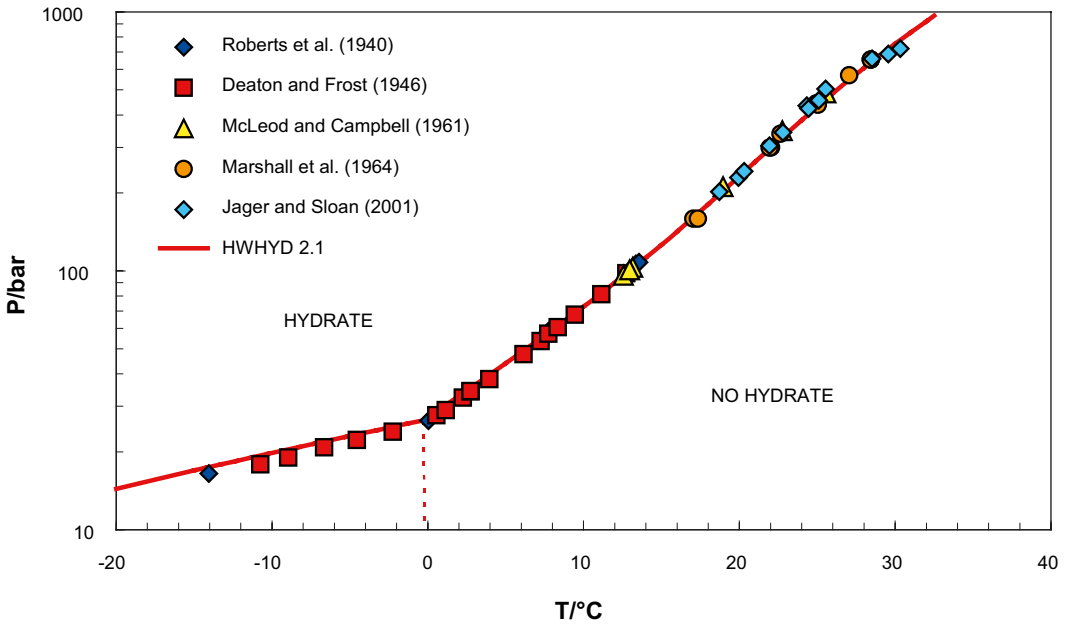

Figure 3-1. *Hydrate stability of methane gas in the presence of distilled water (Gas-Hydrate-Ice and Gas-Hydrate-Water regions) compared with experimental data /Roberts et al. 1940, Deaton and Frost 1946, McLeod and Campbell 1961, Marshall et al. 1964, Jager and Sloan 2001/. Computer code HWHYD 2.1 refers to the second version (cf. Chapter 2).*

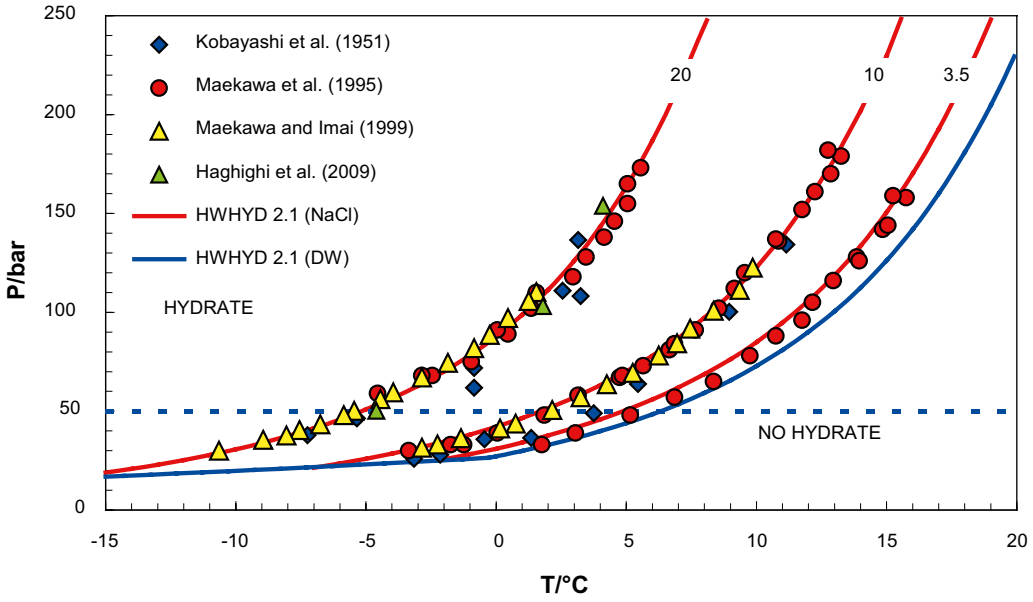

Figure 3-2. *Hydrate stability of methane gas in the presence of various concentrations (wt%) of NaCl (Gas-Hydrate-Ice and Gas-Hydrate-Water regions) compared with experimental data /Kobayashi et al. 1951, Maekawa et al. 1995, Maekawa and Imai 2000, Haghighi et al. 2009/. The hydrostatic pressure corresponding to about 500 m depth is indicated by the blue horizontal line at 50 bar. The curves have been calculated with the HWHYD 2.1 model for the different salinities (NaCl) and distilled water (DW).*

4 Results and Discussions

The hydrate stability zone for methane gas in the presence of various concentrations of salt (NaCl) is presented in Figure 4-1 (assuming excess water). As shown in the figure, the presence of salt shifts the hydrate stability zone to higher pressure or lower temperature conditions.

Figure 4-2 to Figure 4-6 show methane solubility as a function of pressure, temperature and salt concentration The figures show the maximum amount of methane that can be present in the aqueous phase before phase separation and two phase flow.

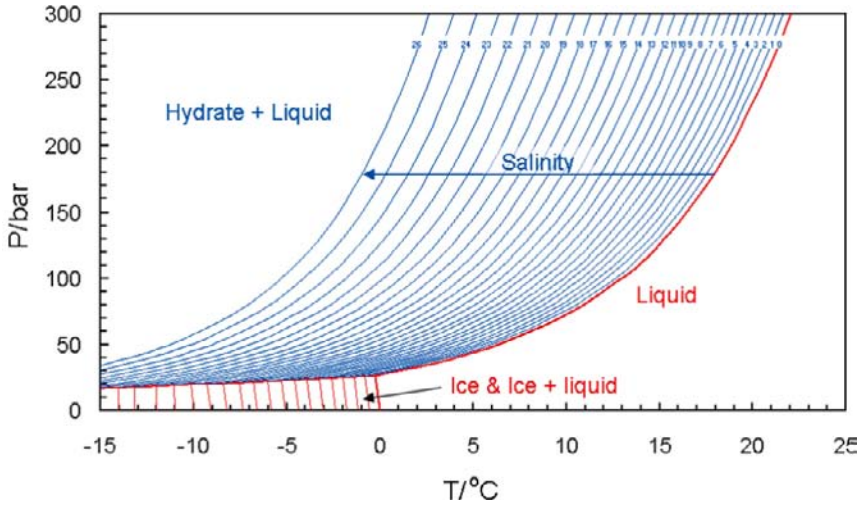

Figure 4-1. *Hydrate stability region for methane in the presence of a gas phase and in the presence of an aqueous phase with various concentrations of salt (weight % of NaCl).*

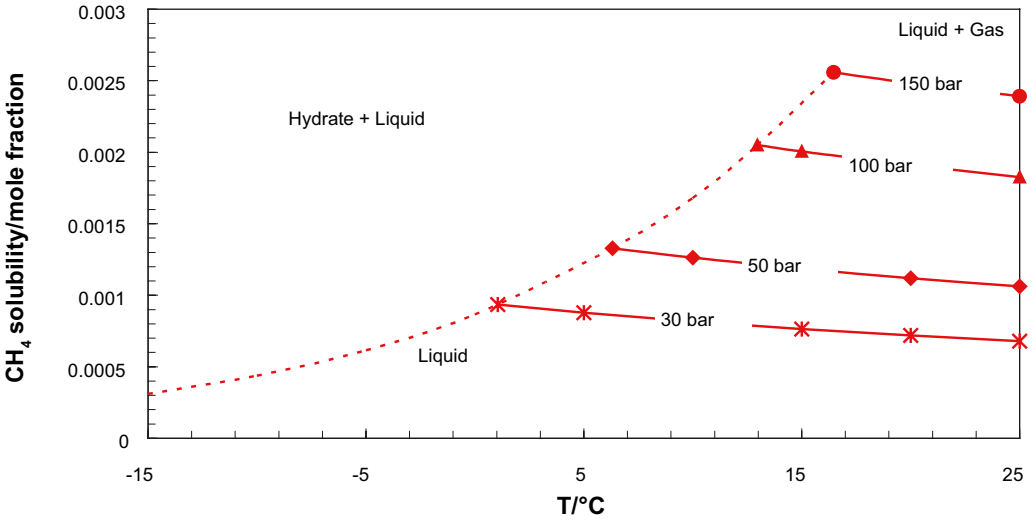

Figure 4-2. *Maximum methane solubility in distilled water (i.e. saturation) as a function of pressure and temperature. Dotted lines represent solubility at 3 phase (gas-hydrate-water) hydrate forming conditions.*

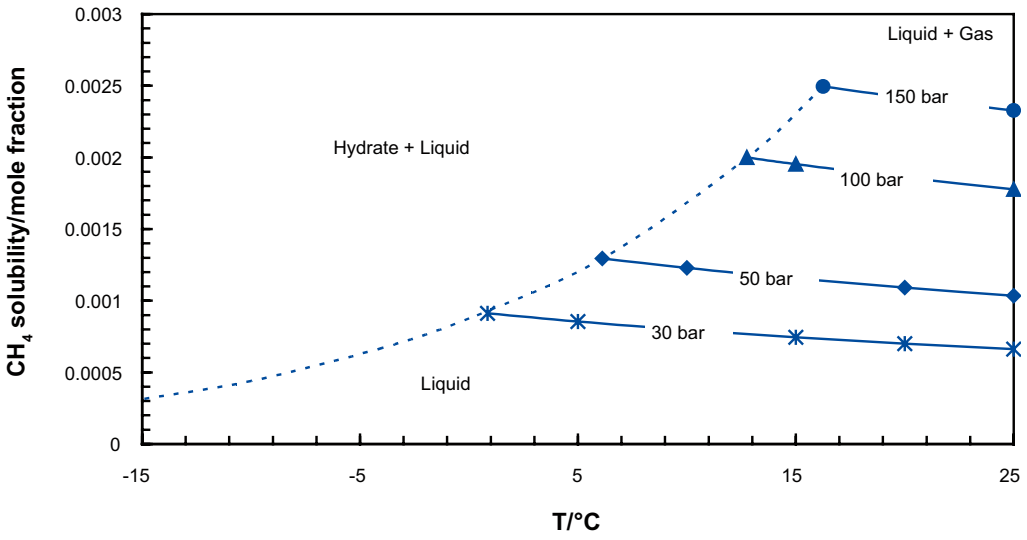

Figure 4-3. *Maximum methane solubility (i.e. saturation) as a function of pressure and temperature in 0.5 mass% NaCl aqueous solution. Dotted lines represent solubility at 3 phase (gas-hydrate-water) hydrate forming conditions.*

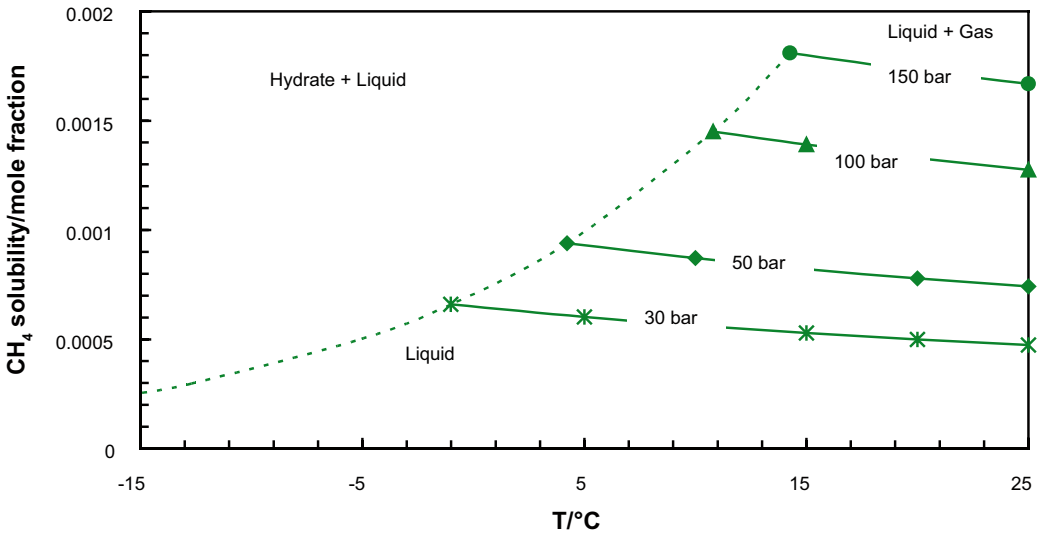

Figure 4-4. *Maximum methane solubility (i.e. saturation) as a function of pressure and temperature in 5 mass% NaCl aqueous solution. Dotted lines represent solubility at 3 phase (gas-hydrate-water) hydrate forming conditions.*

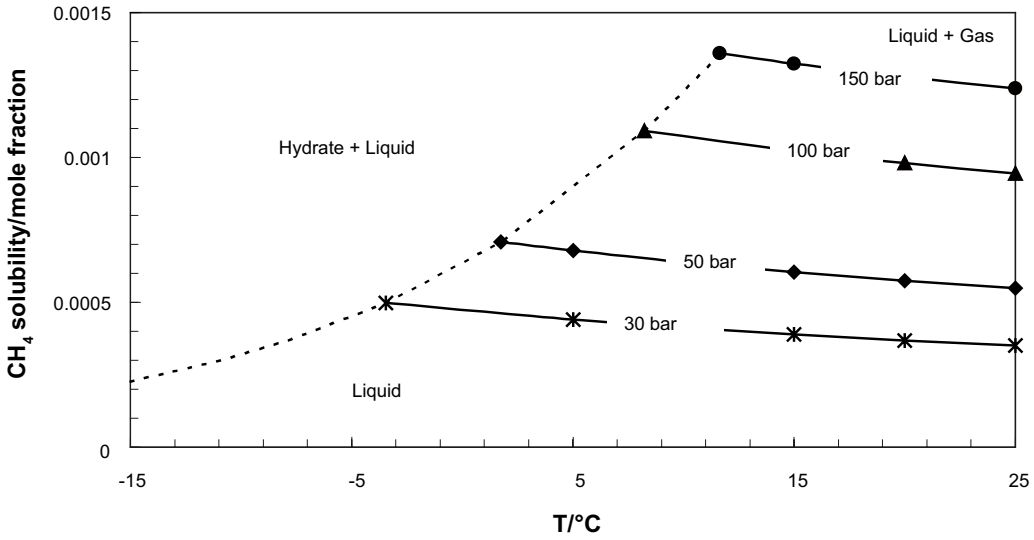

Figure 4-5. *Maximum methane solubility (i.e. saturation) as a function of pressure and temperature in 10 mass% NaCl aqueous solution. Dotted lines represent solubility at 3 phase (gas-hydrate-water) hydrate forming conditions.*

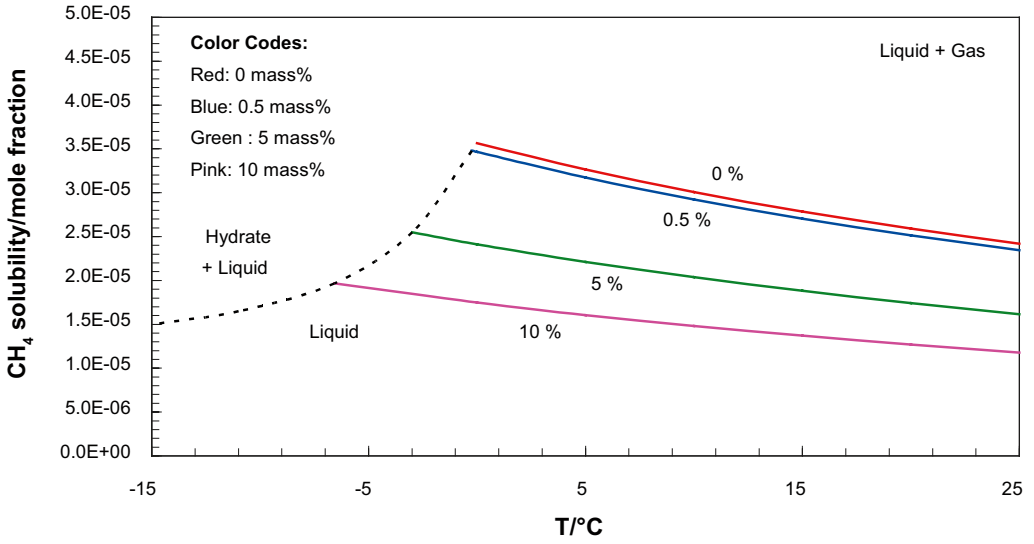

Figure 4-6. *Maximum methane solubility (i.e. saturation) as a function of temperature at 1 bar in the presence of various concentrations of NaCl aqueous solution. Dotted lines represent solubility at ice forming conditions.*

In order to evaluate the potential for hydrate formation as a result of methane gas accumulation under an impermeable layer of permafrost, the methane hydrate stability zone as a function of concentration and dissolved gas and salt concentration has been calculated. The results are presented in Table 4-1 to Table 4-3 and Figure 4-7 to Figure 4-9 for 0.5, 5 and 10 mass% NaCl aqueous solutions, respectively.

Table 4-1. Methane solubility in 0.5 mass% NaCl aqueous solution at the point of hydrate equilibria in the liquid water-hydrate two phase region.

T/°C	0	5	10	15
P_{min}/bar	27.7	44.8	74.3	129.2
CH_4 solubility/mole fraction	0.00086	0.00120	0.00167	0.00231

Table 4-2. Methane solubility in 5 mass% NaCl aqueous solution at the point of hydrate equilibria in the liquid water-hydrate two phase region.

T/°C	0	5	10	15
P_{min}/bar	33.1	54.1	91.5	164.1
CH_4 solubility/mole fraction	0.00071	0.00099	0.00138	0.00189

Table 4-3. Methane solubility in 10 mass% NaCl aqueous solution at the point of hydrate equilibria in the liquid water-hydrate two phase region.

T/°C	-5	0	5	10
P_{min}/bar	25.9	42.1	70.1	122.7
CH_4 solubility/mole fraction	0.00045	0.00063	0.00088	0.00122

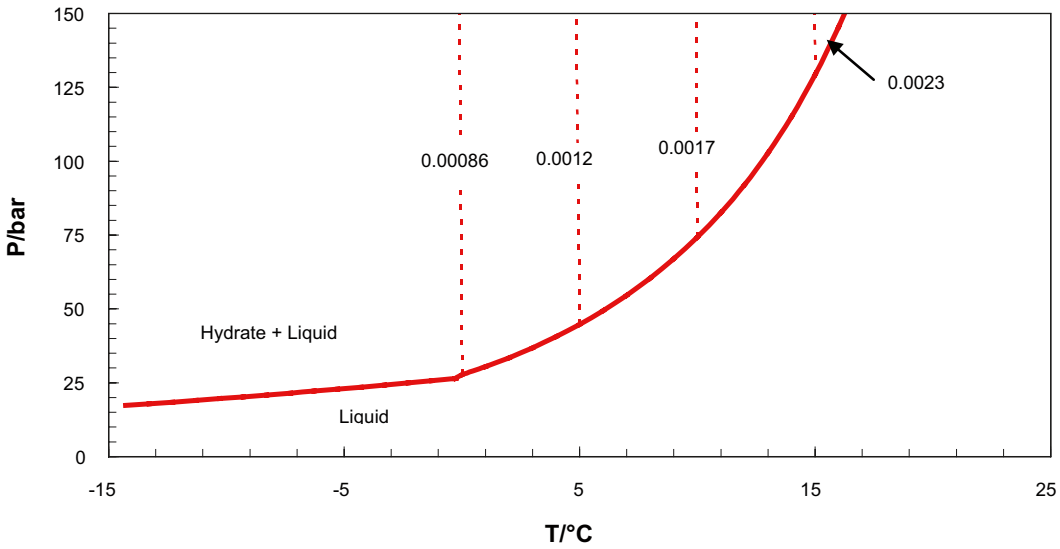

Figure 4-7. *Hydrate stability and iso-solubility (in mole fraction methane dissolved) in 0.5 mass% NaCl aqueous solution. Lower temperature, higher gas content will result in hydrate formation.*

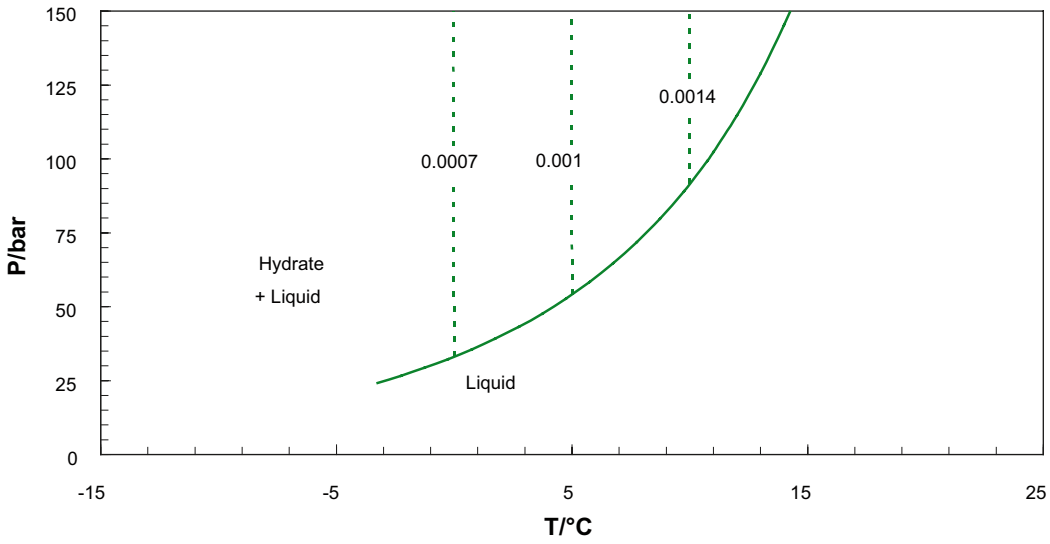

Figure 4-8. *Hydrate stability and iso-solubility (in mole fraction methane dissolved) in 5 mass% NaCl aqueous solution. Lower temperature, higher gas content will result in hydrate formation.*

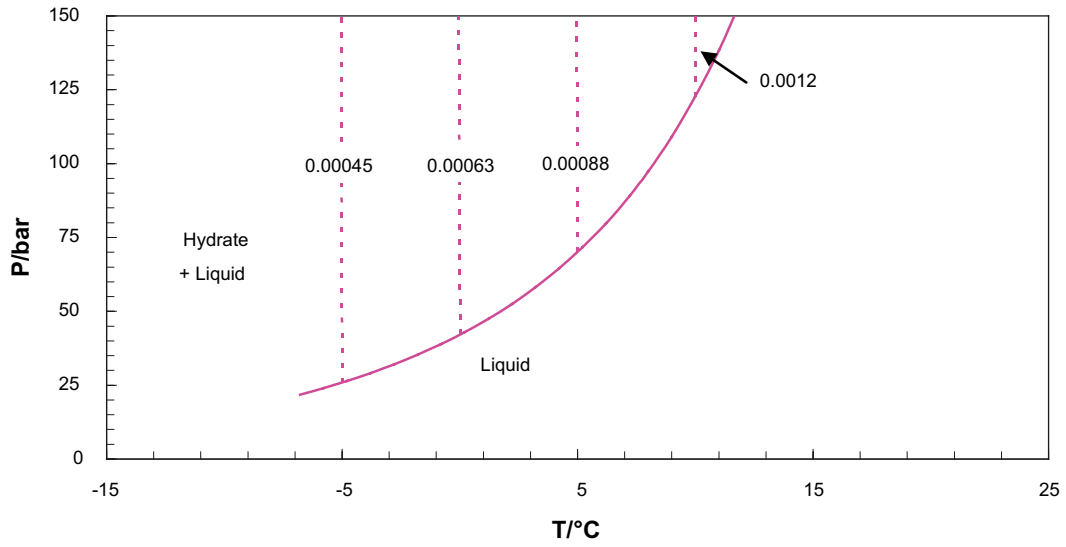

Figure 4-9. *Hydrate stability and iso-solubility (in mole fraction methane dissolved) in 10 mass% NaCl aqueous solution. Lower temperature, higher gas content will result in hydrate formation.*

Figure 4-10 to Figure 4-17 show the hydrate stability temperature as a function of methane gas solubility at constant system pressure of 50, 100, 150, 200, 250, and 300 bar and over a wide range of salt concentrations (i.e. 0-25 mass%).

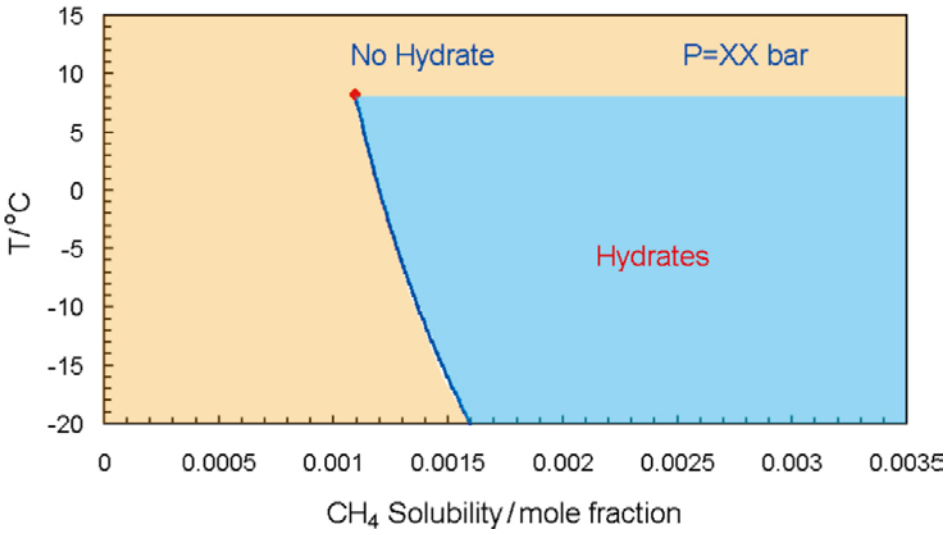

Figure 4-10. *Example of the hydrate stability zone for a given pressure and salinity in the Liquid water-Hydrate two phase region. This figure is provided as guidance on how to interpret the following Figures in this section, where pressures and salinities are specified. The blue zone is the region where hydrates can form, and the orange region is the region where hydrates are not stable because either the temperature is too high or the methane solubility in the aqueous phase is too low.*

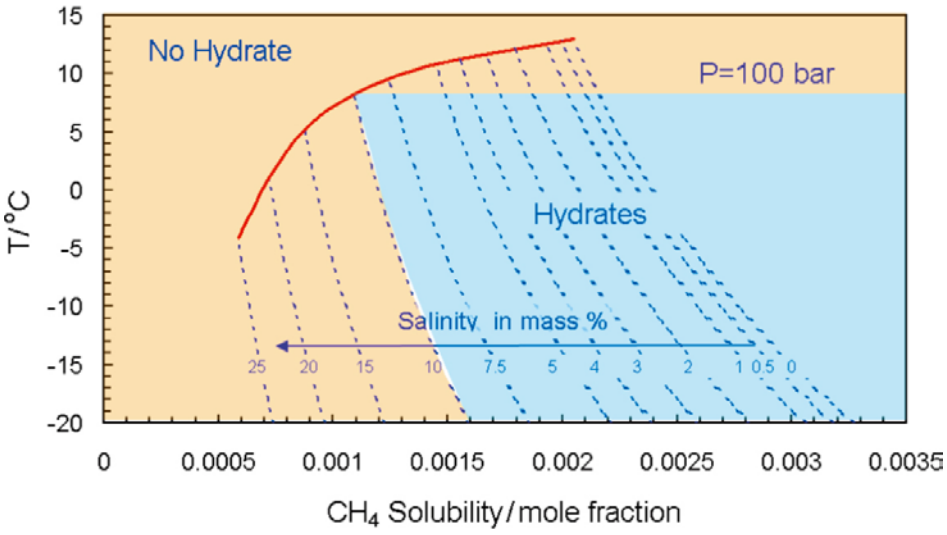

Figure 4-11. *Hydrate stability zone for methane hydrates (dissolved gas, i.e. Liquid water-Hydrate two phase region) in the presence of 0-25 mass% salt concentration at 100 bar. As an example for 10 mass% NaCl at 100 bar, the blue zone is the region where hydrates can form, and the orange region is the region where hydrates are not stable because either the temperature is too high (if T > 8°C) or the methane solubility in the aqueous phase is too low.*

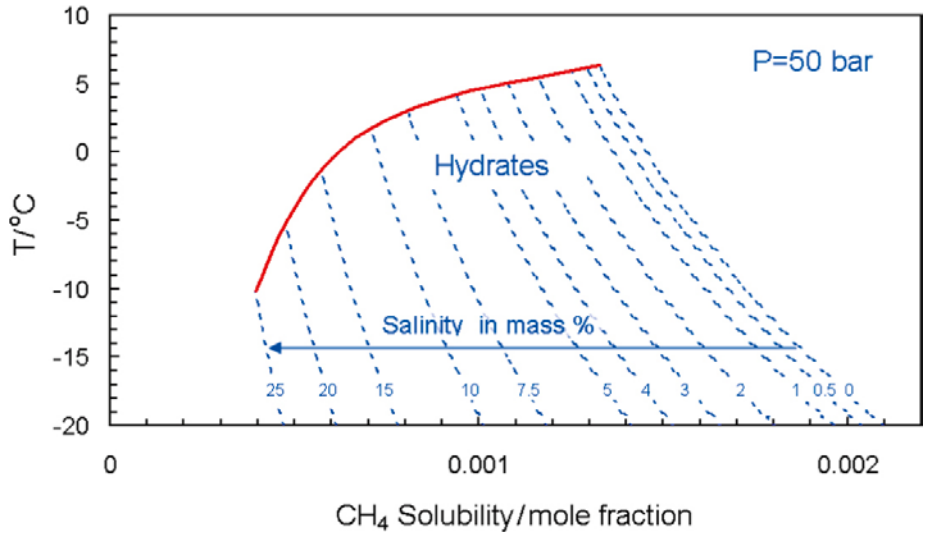

Figure 4-12. *Hydrate stability temperature as a function of methane solubility (in the Liquid water-Hydrate two phase region) at 50 bar and at various NaCl concentrations.*

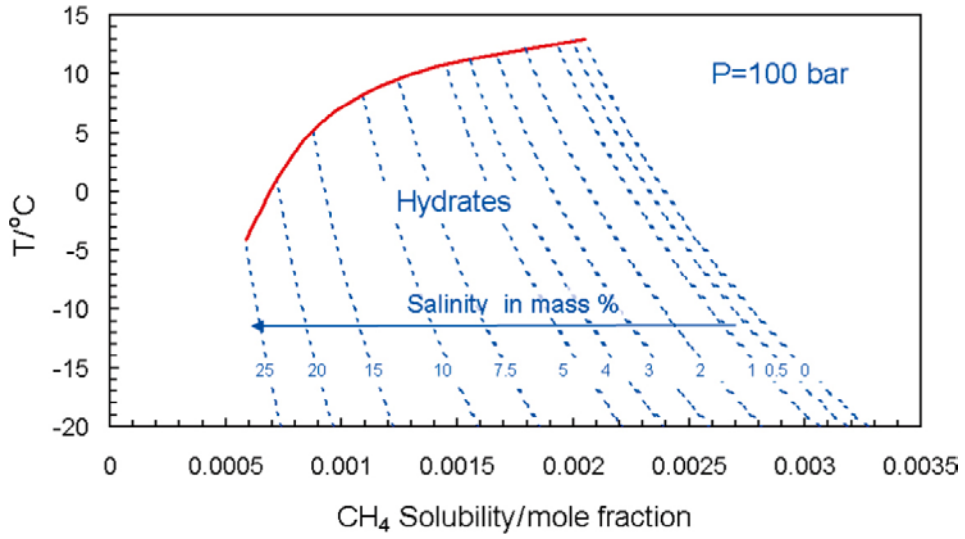

Figure 4-13. *Hydrate stability temperature as a function of methane solubility (in the Liquid water-Hydrate two phase region) at 100 bar and at various NaCl concentrations.*

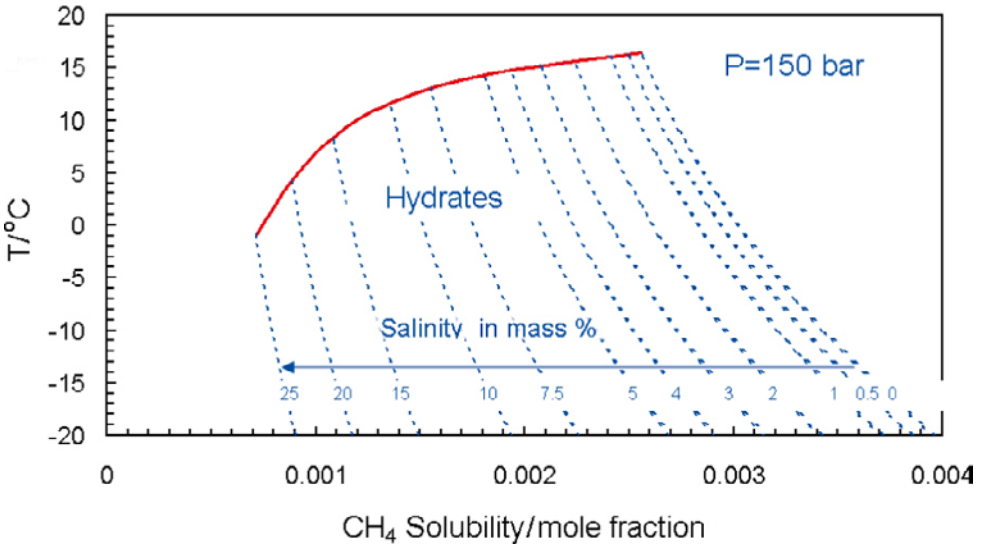

Figure 4-14. *Hydrate stability temperature as a function of methane solubility (in the Liquid water-Hydrate two phase region) at 150 bar and at various NaCl concentrations.*

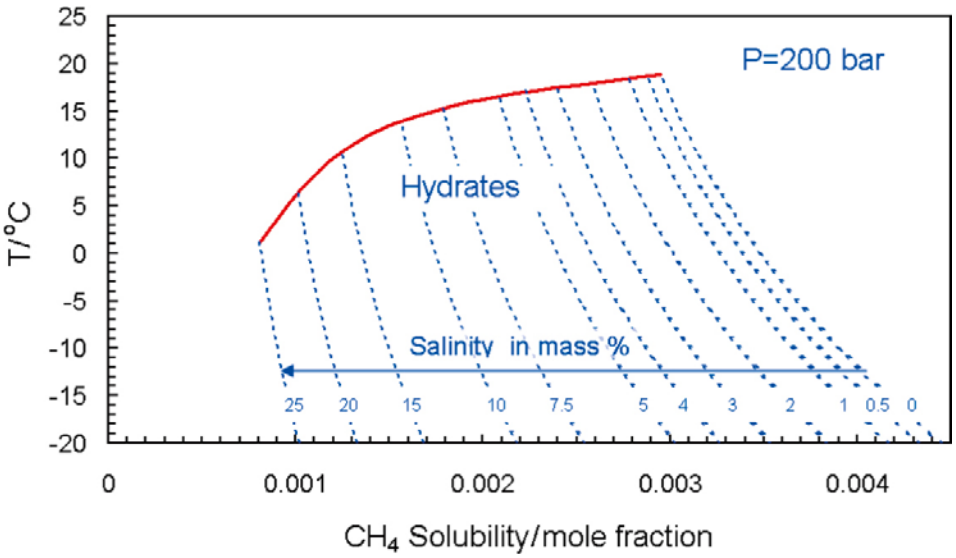

Figure 4-15. *Hydrate stability temperature as a function of methane solubility (in the Liquid water-Hydrate two phase region) at 200 bar and at various NaCl concentrations.*

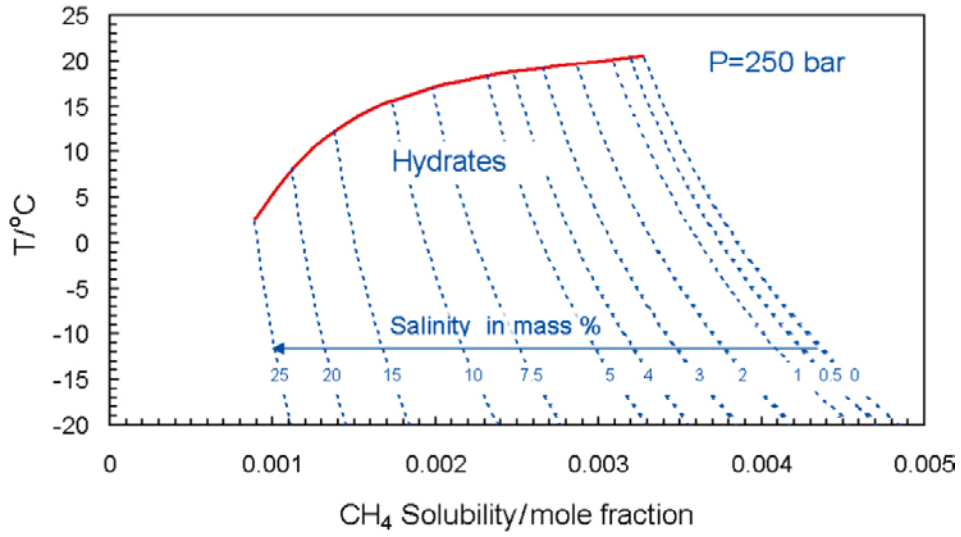

Figure 4-16. *Hydrate stability temperature as a function of methane solubility (in the Liquid water-Hydrate two phase region) at 250 bar and at various NaCl concentrations.*

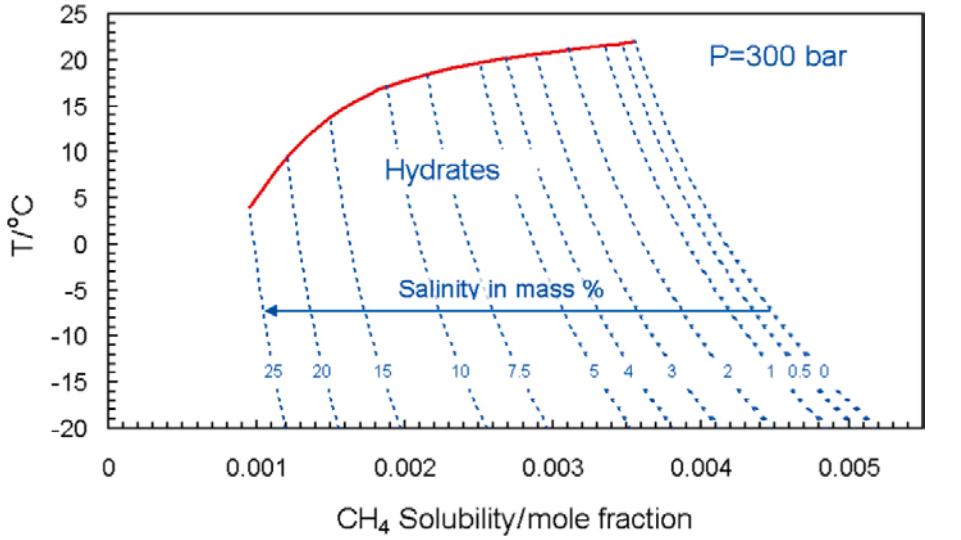

Figure 4-17. *Hydrate stability temperature as a function of methane solubility (in the Liquid water-Hydrate two phase region) at 300 bar and at various NaCl concentrations.*

Figure 4-18 summarises the results obtained in this section. Using this figure it is possible to assess the maximum temperature and minimum pressure needed for methane hydrates to be formed from an aqueous solution with given methane and salt concentrations.

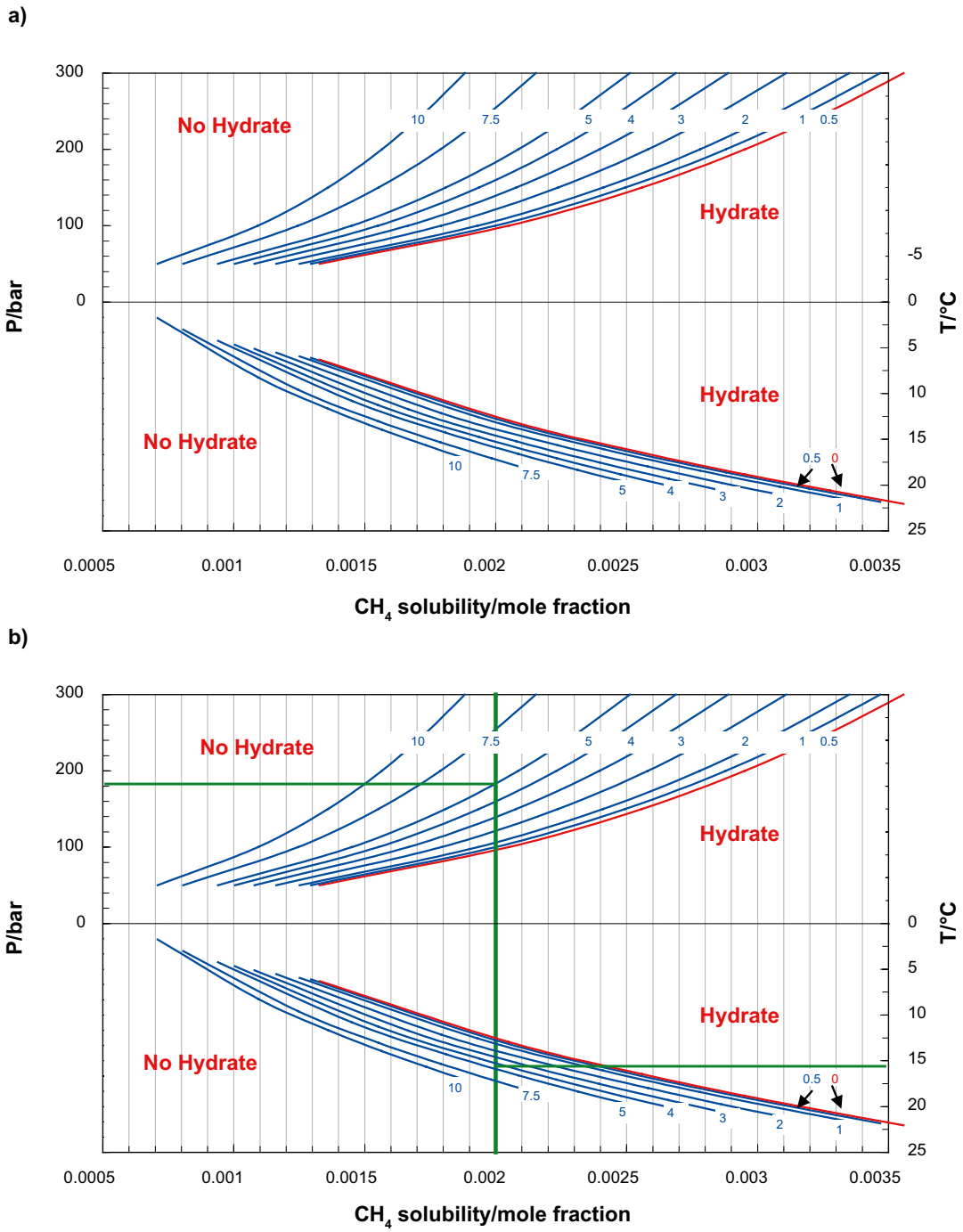

Figure 4-18. *a) Hydrate stability temperature as a function of methane solubility and at various NaCl concentrations. b) How to determine if hydrates are stable? For example, if the methane concentration is 0.002 (mole fraction) and the salinity is 5 mass%, is it possible to show that the temperature and pressure at which hydrates are stable? In this example the temperature must be lower than 16°C and the pressure lower than 190 bar.*

5 Relevance to Swedish and Finnish sites

Field data available from the Forsmark and Laxemar sites in Sweden /Hallbeck and Pedersen 2008a, b, Laaksoharju et al. 2008a, b, 2009/ are shown in Figure 5-1 and Figure 5-2, and the data for the Olkiluoto site in Finland is shown in Figure 5-3 and in Figure 5-4 /Pitkänen et al. 2004/. Using these data, the possibility of hydrate formation for some typical NaCl and methane concentrations was analysed.

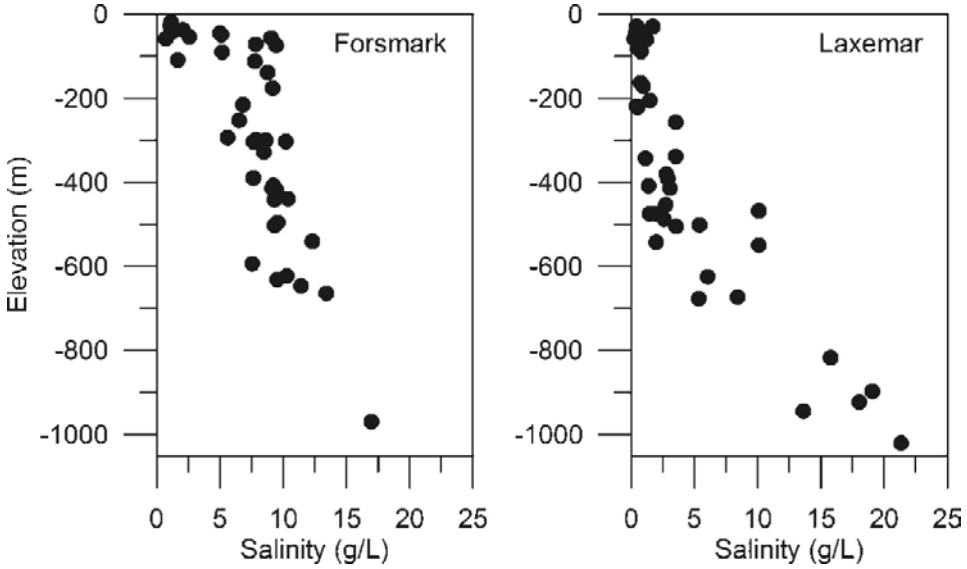

Figure 5-1. *Typical salt concentrations in the groundwaters sampled at the Forsmark and Laxemar sites in Sweden /Laaksoharju et al. 2008a, b, 2009/. For Forsmark the maximum salt concentration is ~1.7 mass% at 1,000 m depth, while at Laxemar the maximum salt concentration is ~2 mass% at 1,000 m depth.*

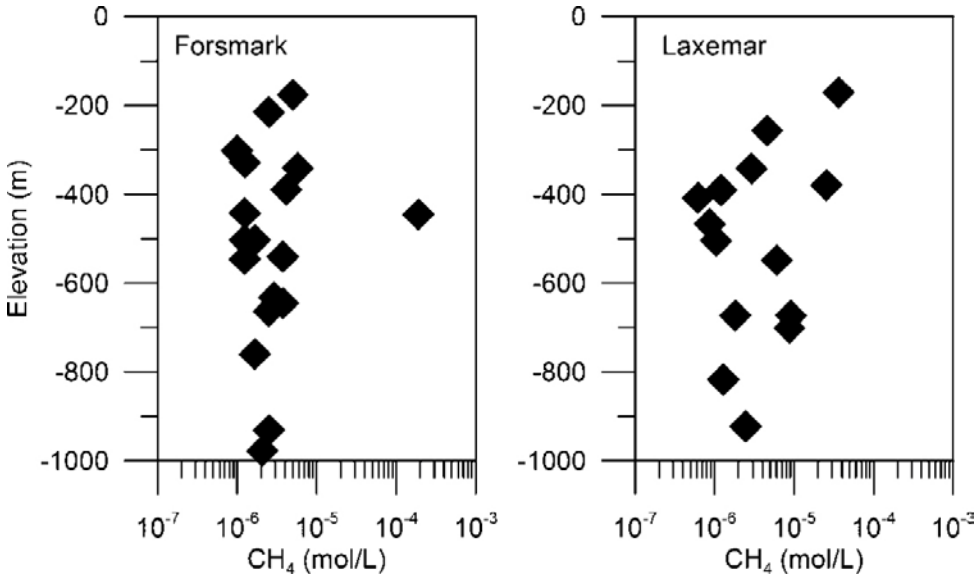

Figure 5-2. *Methane concentrations in groundwaters for the Swedish sites investigated by SKB /Hallbeck and Pedersen 2008a, b/.*

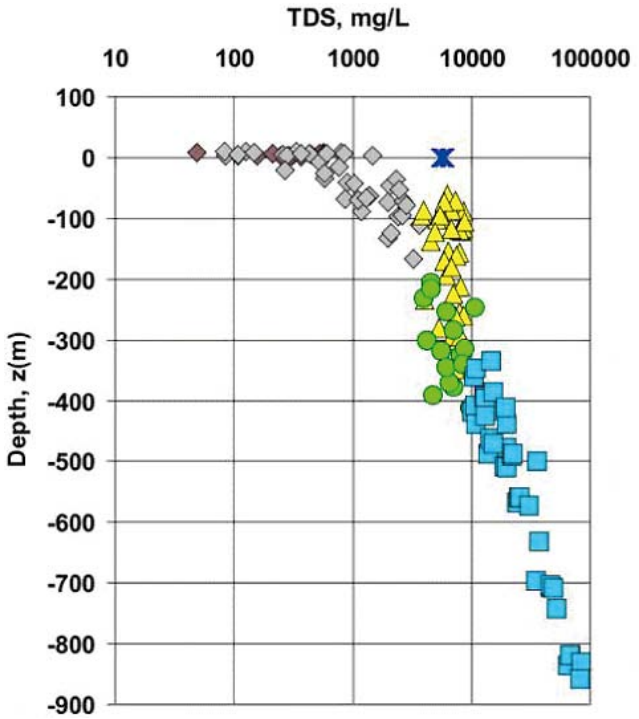

Figure 5-3. *Salt concentrations (total dissolved solids, TDS) in the groundwaters at Olkiluoto, Finland /Pitkänen et al. 2004/. The maximum salinities are ~10 mass% at 900 m depth. Dark blue symbol represents present day Baltic Sea salinity at Olkiluoto.*

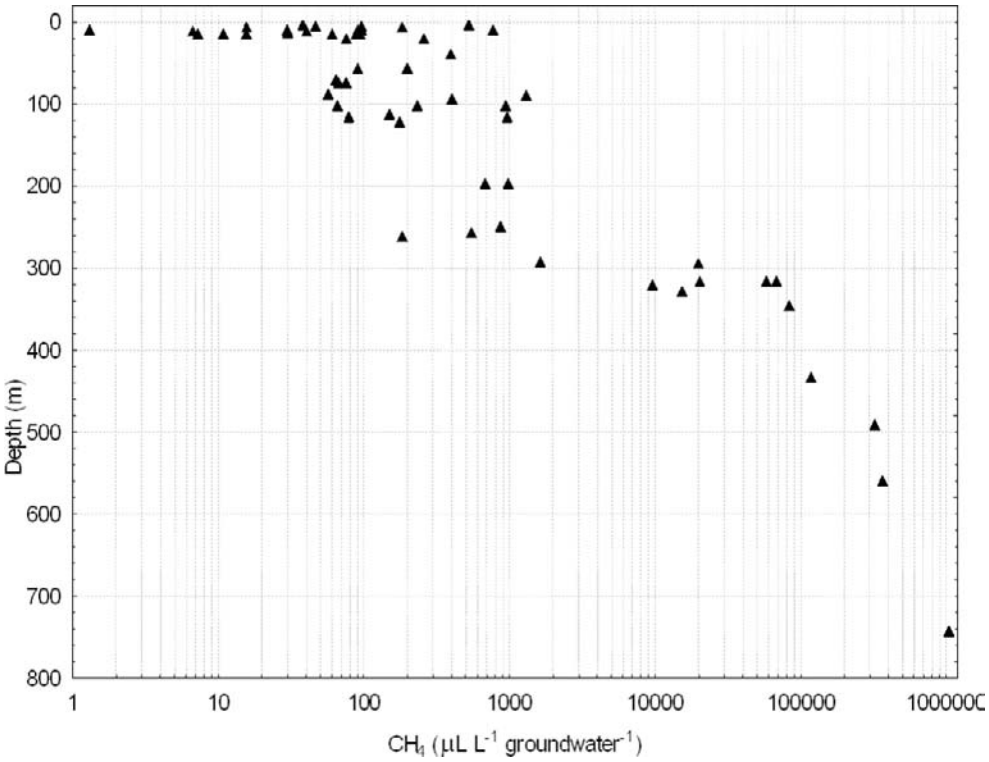

Figure 5-4. *Methane concentrations in the groundwaters at Olkiluoto, Finland /Pitkänen et al. 2004/. Maximum methane concentration: ~4x10^{-2} mol/L, i.e. ~7.3x10^{-4} mole fraction.*

Figure 5-5 shows the hydrate stability pressure as a function of gas solubility at various salt concentrations. The figure shows that at the maximum CH_4 content in the groundwaters from Olkiluoto (~0.00073 mole fraction) and at the corresponding salinity of 10 mass% NaCl, the stability pressure for the hydrate is ≤ 50 bar, and therefore the groundwater pressure at the corresponding depth (~100 bar) in Olkiluoto lies outside the hydrate stability zone.

The high methane concentrations at Olkiluoto represent the worst case for hydrate formation among the sites discussed here (greatest methane concentration: $\sim 4\times10^{-2}$ mol/L $\sim 7.3\times10^{-4}$ mole fraction). At 500 m depth at Olkiluoto, Figure 5-4 shows that the methane concentration is ~0.35 L_{CH4}/L_{water}, which corresponds to ~0.00025 mole fraction, and in order to be inside the hydrate stability region, Figure 4-12 shows that the salinity needs to be larger than 25% and the temperature below −10°C at the hydrostatic pressure prevailing at that depth, 50 bar.

At greater depths at Olkiluoto, i.e. at 1,000 m where the hydrostatic pressure is 100 bar, the methane concentration and salinity increases, the methane mole fraction is up to ~0.00073 and the salinity almost up to 10%. Figure 4-13 shows that to be inside the hydrate stability zone, the salinity needs to be higher than 20 mass% and the temperate below ~5°C. This is also illustrated in Figure 4-18 and in Figure 5-5. The required combination of pressure, NaCl and methane to be inside the hydrate stability zone is not encountered at the site.

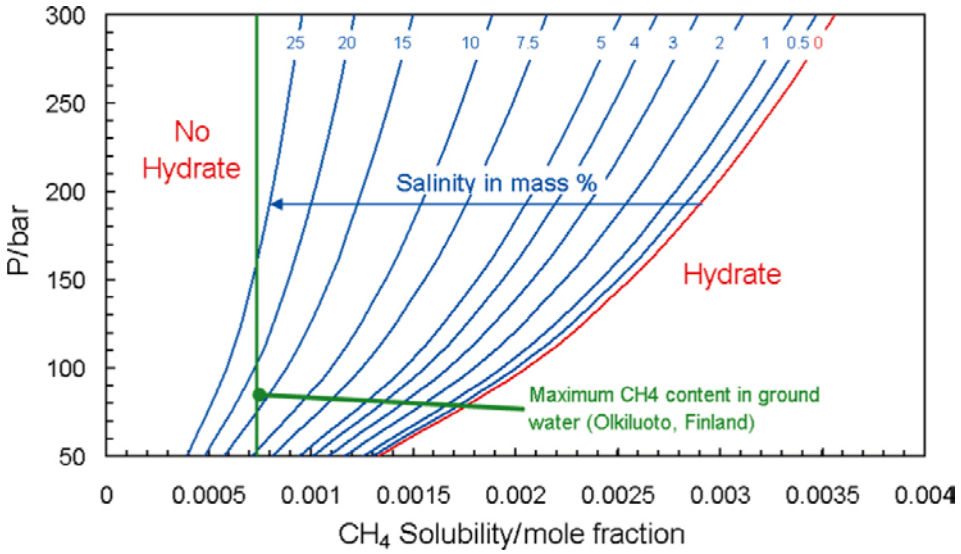

Figure 5-5. *Hydrate stability pressure as a function of gas solubility at various salt concentrations.*

6 Time scales for methane hydrate accumulation in the Swedish and Finnish sites

The model presented in /Rempel and Buffett 1997/ indicates hundreds of thousands of years for the formation of methane hydrate layers. In /Bath and Hermansson 2009/ the authors estimate a CH_4 flux at Olkiluoto of $\sim 3.6 \times 10^{-10}$ mol m^{-2} yr^{-1} and from this value they show that it would take many millions of years to create a 500 metre thick layer of methane hydrates.

The flow of methane at Olkiluoto has been evaluated within the SR-Site project /Delos et al. 2010/ to 1.9×10^{-7} mol m^{-2} yr^{-1}. For the Swedish sites of Forsmark and Laxemar the flows of methane are some orders of magnitude lower. An estimate of the time needed to create a layer of methane hydrate may be obtained using this, hopefully more accurate, value.

As an example, 0.2% of the rock volume is taken to be available for hydrate formation. The density of the hydrate is 913.4 kg/m^3 (cf. Appendix) and the formula of the hydrate is $CH_4 \cdot 6.25H_2O$. The data and the methane flow indicate that very long periods of time would be required for CH_4 to be transported to the depth where temperature and pressure conditions could be favourable for hydrate formation. For example, it may be calculated that a 1 m thick hydrate layer requires $\sim 75 \times 10^6$ yr to be formed.

7 Conclusions

The main aim of this work was to establish whether the pertaining pressure and temperature conditions and dissolved gas concentration in groundwater is conducive to gas hydrate formation using a modelling investigation.

The computer simulations for determining the hydrate stability zone of dissolved methane in the presence of salt, show that a decrease in the system pressure and/or an increase in salt concentration favours hydrate formation, as both factors reduce equilibrium gas solubility in the aqueous phase. This behaviour is unlike that of the system including a gas phase, where a higher gas pressure corresponds to an increased gas solubility which favours hydrate formation.

The main conclusion is that at the site where the conditions are most favourable for methane hydrate formation, Olkiluoto in Finland, the methane concentrations, salinities and prevailing hydrostatic pressures are outside the zone of methane hydrate stability even for future periglacial (permafrost) conditions when temperatures at repository depths, about 500 m, are expected to become close to 0°C for some periods of time /SKB 2010/.

In addition, the simulation provides the necessary data to estimate the effect of increase in dissolved methane concentration on potential hydrate formation, as well as two phase flow.

Furthermore, small diffusive flows of methane are calculated elsewhere /Delos et al. 2010/ from the observed methane concentration gradients with depth at the Swedish and Finnish sites studied. These calculated flows indicate that it would take many millions of years of favourable conditions for hydrate formation in order to accumulate enough methane to form even a thin layer of hydrate.

8 References

SKB's (Svensk Kärnbränslehantering AB) publications can be found at www.skb.se/publications.

Avlonitis D, Danesh A, Todd A C, 1994. Prediction of VL and VLL equilibria of mixtures containing petroleum reservoir fluids and methanol with a cubic EoS. Fluid Phase Equilibria, 94, pp 181–216.

Bath A, Hermansson H-P, 2009. Biogeochemistry of redox at repository depth and implications for the canister. SSM Report 2009:28, Strålsäkerhetsmyndigheten (Swedish Radiation Safety Authority).

Chapoy A, Mohammadi A H, Richon D, Tohidi B, 2004. Gas solubility measurement and modeling for methane–water and methane–ethane–n-butane–water systems near hydrate forming conditions. Fluid Phase Equilibria, 220, pp 111–119.

Dallimore S R, Collett T S, 1995. Intrapermafrost gas hydrates from a deep core hole in the Mackenzie Delta, Northwest Territories, Canada. Geology, 23, pp 527–530.

Dallimore S R, Collett T S, 1999. Regional hydrate occurrences, permafrost conditions, and Cenozoic geology, MacKenzie Delta area. In: Dallimore S R, Uchida T, Collett T S (eds). Scientific Results from the JAPEX/JNOC/GSC Mallik 2L-38 Gas Hydrate research Well, MacKenzie Delta, Northwest Yerritories, Canada. Geological Survey of Canada Bulletin, 544, pp 31–43.

Deaton W M, Frost E M, 1946. Gas hydrate composition and equilibrium data. Oil and Gas Journal, 45, pp 170–178.

Delos A, Dentz M, Trinchero P, Pitkänen P, Richard L, Molinero J, 2010. Quantitative assessment of deep gas migration in Fennoscandian sites. SKB R-10-61, Svensk Kärnbränslehantering AB.

Haghighi H, Chapoy A, Tohidi B, 2009. Methane and Water Phase Equilibria in the Presence of Single and Mixed Electrolyte Solutions Using the Cubic-Plus-Association Equation of State. Oil & Gas Science and Technology – Revue d'IFP Energies nouvelles, 64, pp 141–154.

Hallbeck L, Pedersen K, 2008a. Explorative analysis of microbes, colloids and gases. SDM-Site Forsmark. SKB R-08-85, Svensk Kärnbränslehantering AB.

Hallbeck L, Pedersen K, 2008b. Explorative analysis of microbes, colloids, and gases together with microbial modelling. Site description model, SDM-Site Laxemar. SKB R-08-109, Svensk Kärnbränslehantering AB.

Holder G D, Corbin G, Papadopoulos K D, 1980. Thermodynamic and molecular properties of gas hydrate from mixtures containing methane, argon and krypton. Industrial and Engineering Chemical Fundamentals, 19, pp 282–286.

Jager M D, Sloan E D, 2001. The effect of pressure on methane hydration in pure water and sodium chloride solutions. Fluid Phase Equilibria, 185, pp 89–99.

Kihara T, 1953. Virial coefficient and models of molecules in gases. Reviews of Modern Physics, 25, pp 831–843.

Kobayashi R, Withrow H J, Williams G B, Katz D L, 1951. Gas hydrate formation with brine and ethanol solutions. Proceedings of the 30th Annual Convention, Natural Gasoline Association of America, USA, pp 27–31.

Laaksoharju M, Smellie J, Tullborg E-L, Gimeno M, Molinero J, Gurban I, Hallbeck L, 2008a. Hydrogeochemical evaluation and modelling performed within the Swedish site investigation programme. Applied Geochemistry, 23, pp 1761–1795.

Laaksoharju M, Smellie J, Tullborg E-L, Gimeno M, Hallbeck L, Molinero J, Waber N, 2008b. Bedrock hydrogeochemistry Forsmark. Site descriptive modelling, SDM-Site Forsmark. SKB R-08-47, Svensk Kärnbränslehantering AB.

Laaksoharju M, Smellie J, Tullborg E-L, Wallin B, Drake H, Gascoyne M, Gimeno M, Gurban I, Hallbeck L, Molinero J, Nilsson A-C, Waber N, 2009. Bedrock hydrogeochemistry Laxemar. Site descriptive model, SDM-Site Laxemar. SKB R-08-93, Svensk Kärnbränslehantering AB.

Maekawa T, Imai N, 2000. Equilibrium conditions of methane and ethane hydrates in aqueous electrolyte solutions. In: Holder G D, Bishnoi P R (eds). Gas hydrates: challenges for the future: proceedings of the third International Conference on Gas Hydrates, Salt Lake City, USA, July 1999. New York: New York Academy of Sciences. (Annals of the New York Academy of Sciences 912)

Maekawa T, Itoh S, Sakata S, Igari S-I, Imai N, 1995. Pressure and temperature conditions for methane hydrate dissociation in sodium chloride solutions. Geochemical Journal, 29, pp 325–329.

Marshall D R, Saito S, Kobayashi R, 1964. Hydrates at high pressures: Part I. Methane-water, argon-water, and nitrogen-water systems. AIChE Journal, 10, pp 202–205.

McLeod H O, Campbell J M, 1961. Natural gas hydrates at pressures to 10,000 psia. Journal of Petroleum Technology, 13, pp 590–594.

Mohammadi A H, Chapoy A, Richon D, Tohidi B, 2004. Experimental measurement and thermodynamic modeling of water content in methane and ethane systems. Industrial & Engineering Chemistry Research, 43, pp 7148–7162.

Najibi H, Chapoy A, Haghighi H, Tohidi B, 2009. Experimental determination and prediction of methane hydrate stability in alcohols and electrolyte solutions. Fluid Phase Equilibria, 275, pp 127–131.

Parrish W R, Prausnitz J M, 1972. Dissociation pressures of gas hydrates formed by gas mixtures. Industrial & Engineering Chemistry Process Design and Development, 11, pp 26–35.

Pitkänen P, Partamies S, Luukkonen A, 2004. Hydrogeochemical interpretation of baseline groundwater conditions at the Olkiluoto site. Posiva 2003-07, Posiva Oy, Finland.

Rempel A W, Buffett B A, 1997. Formation and accumulation of gas hydrate in porous media. Journal of Geophysical Research, 102, pp 10151–10164.

Roberts O L, Brownscombe E R, Howe L S, 1940. Constitution diagrams and composition of methane and ethane hydrates. Oil and Gas Journal, 39, pp 37–43.

SKB, 2010. Climate and climate related issues for the safety assessment SR-Site. SKB TR-10-49, Svensk Kärnbränslehantering AB.

Valderrama J O, 1990. A generalized Patel-Teja equation of state for polar and non-polar fluids and their mixtures. Journal of Chemical Engineering of Japan, 23, pp 87–91.

van der Waals J H, Platteeuw J C, 1959. Clathrate solutions. In: Prigogine I (ed). Advances in Chemical Physics. Vol. 2. New York: Interscience, pp 1–57.

Data and Conversion Factors

Molecular weight
W_{CH_4} = 16.043 g/mol, W_{H_2O} = 18.0153 g/mol.

Volume
Methane Volume (273.15 K, 1 bar) STP: 22.65775 Litre/mol.

Water Volume at IUPAC (273.15 K, 1 bar) STP: 0.018018 Litre/mol.

Density
Ice: 916.7 kg/m^3; Methane hydrate: 913.43 kg/m^3.

Concentration
Methane mole fraction: $x_{CH_4} = \dfrac{n_{CH_4}}{n_{CH_4} + n_{H_2O}}$

where n_i is the number of moles of component *"i"*. To obtain the mole fraction of methane in a solution with a given salinity and concentration of methane:

$$x_{CH_4} = \frac{m_{CH_4}}{m_{CH_4} + 2m_{NaCl} + 1000 / W_{H_2O}}$$

where m_i is the moles of the *"i"* solute per kg of H_2O (molality). For example, a solution with $m_{CH_4} = 1\times10^{-4}$ mol/(kg H_2O) and negligible salinity has $x_{CH_4} = 1.80\times10^{-6}$, while if the salinity is 10 weight % (m_{NaCl} = 1.9 mol/(kg H_2O)) then $x_{CH_4} = 1.74\times10^{-6}$.

For dilute aqueous solutions at low temperatures (below 25°) there is little difference between the concentration in molality units (moles per kg of H_2O) and molarity units (moles per litre of aqueous solution) because the density is close to 1 g/mL. If the density, d, of the aqueous solution is known, the conversion between molarity, c_i, and molality, m_i, is given by:

$$m_i = \frac{c_i}{d - 0.001\, c_i\, W_i} \qquad c_i = \frac{m_i\, d}{1 + 0.001\, m_i\, W_i}$$

For example, a NaCl solution with c_{NaCl} = 1.84 mol/L, with d = 999.7 kg/m^3 at 0°C, has m_{NaCl} = 1.901 mol/(kg H_2O).

The conversion from weight % to molality (moles per kg H_2O) is given by:

$$m_i = \frac{1000\,\%}{(100 - \%)\, W_i}$$

For example, 1 weight % NaCl corresponds to m_{NaCl} = 0.173 mol/(kg H_2O); while the m_{NaCl} = 1.901 mol/(kg H_2O) solution in the previous example has 10 weight % of NaCl.

When gas concentrations are reported as volume of gas per litre of groundwater, for example in Figure 5-4, the conversion may be made knowing that the molar volume of CH_4 is, as listed above, 22.658 L/mol at 0°C and 1 bar. For example, a CH_4 concentration of 0.35 L_{CH4}/L_w has $c_{CH_4} \approx$ 0.015 mol/L and $x_{CH_4} \approx 2.7\times10^{-4}$. In general it is not clear to what temperature the gas volume corresponds, and at other temperatures the molar volume may be corrected as follows: ~ (22.658 L/mol × (273.15 + t°C) / 273.15).